
Distilling Conditional Diffusion Models for Offline Reinforcement Learning through Trajectory Stitching

Shangzhe Li^{1,2} Xinhua Zhang³

Abstract

Deep generative models have recently emerged as an effective approach to offline reinforcement learning. However, their large model size poses challenges in computation. We address this issue by proposing a knowledge distillation method based on data augmentation. In particular, high-return trajectories are generated from a conditional diffusion model, and they are blended with the original trajectories through a novel stitching algorithm that leverages a new reward generator. Applying the resulting dataset to behavioral cloning, the learned shallow policy whose size is much smaller outperforms or nearly matches deep generative planners on several D4RL benchmarks.

1. Introduction

Offline reinforcement learning (RL) presents a novel opportunity to leverage offline batch data without having to interact with the environment (Levine et al., 2020). Simple approaches such as Behavioral Cloning (BC) are directly applicable, minimizing the error between the target policy and the learned policy. However, both BC and many well-established *online* RL methods suffer from the out-of-distribution (OOD) issues because once deployed online, the state distribution can shift considerably from that in the offline data, and the Q-value can be over-estimated on OOD states-actions (Fujimoto et al., 2019; Kumar et al., 2019; Fu et al., 2019; Kumar et al., 2020a).

A large number of methods have been proposed to address this issue, and we only highlight a few. Kumar et al. (2020b) proposed conservative Q-learning (CQL) to pessimistically under-estimate the state-action values for OOD actions. Nair et al. (2020) and several other works constrain the policy to

the proximity of the behavior policy. Implicit Q-learning (IQL, Kostrikov et al., 2021) avoids querying values of unseen actions while performing multi-step dynamic programming updates.

Recently, methods based on large generative models have showed significant promise on a number of synthetic and real-world RL tasks, e.g., Decision Transformer (DT, Chen et al., 2021), Diffusion Q-learning (Wang et al., 2023b), and Decision Diffuser (DD, Ajay et al., 2023). DT and trajectory transformer (Janner et al., 2021b) train a transformer to model the policy or the planning algorithm. DD trains a *conditional* diffusion model to generate high-return trajectories, which empowers effective planning, even if there are not many high-return trajectories in the original data.

However, since these deep generative models contain a large volume of parameters, applying them to online decision making demands substantial computational power, which is difficult to meet in many practical devices such as the light-weight processors carried by robots. A common wisdom is to distill/compress the large model without significantly degrading the performance (Hinton et al., 2015). Ideally, we aim to directly represent the policy network by a shallow model without running deep diffusions or multi-head attentions, dispensing with expensive online planning.

A direct method to distill a policy is based on matching the actions with the offline transitions, which unfortunately suffers the same issues plaguing BC. To improve the performance of BC, Hepburn & Montana (2023) recently proposed Model-Based trajectory Stitching (MBTS), which augments the offline dataset by stitching high-value regions of different trajectories. However, MBTS only stitches existing trajectories while not generating new high-return trajectories, leaving the stitched dataset still sub-optimal.

Motivated by MBTS, we propose pursuing another path of knowledge distillation via data augmentation. In particular, we may use the large generative models such as conditional diffusers to generate new high-return trajectories, which are then used to augment the dataset by stitching with the original trajectories.

Our Trajectory Stitching Knowledge Distilling (TSKD) algorithm does not simply add the high-return conditioned

¹School of Future Technology, South China University of Technology, Guangzhou, China ²Department of Informatics, Technical University of Munich, Munich, Germany ³Department of Computer Science, University of Illinois Chicago, Chicago, USA. Correspondence to: Shangzhe Li <shangzhe.li@tum.de>, Xinhua Zhang <zhangx@uic.edu>.

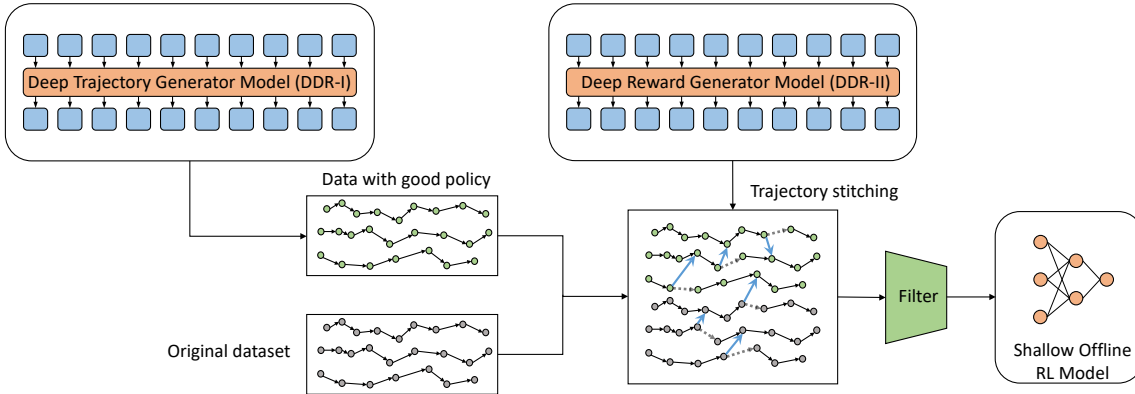


Figure 1. The Trajectory Stitching Knowledge Distilling (TSKD) method. Trajectories generated by DDR-I are combined with the original dataset for the stitching process, which creates new transitions (blue arrows in the “Trajectory stitching” block) and discards old transitions (grey dotted edges). A reward is generated by DDR-II during stitching. A filter is applied to prune away low-return trajectories based on a threshold. The result is finally used to train a shallow BC model.

trajectories for BC training, because this would potentially overfit high-value regions and lead to OOD issues for BC. Instead, they are blended into the original dataset progressively with a selective stitching strategy, which introduces new transitions between two states on two different trajectories. Secondly, generation from conditional diffusers can be computationally expensive, making it more efficient to only extract a small number of trajectories from it, supplemented by a larger number of trajectories based on the cheaper process of stitching with the original dataset. Finally, stitching allows us to downweight or even discard the subsequences that correspond to a poor policy – once a state from trajectory τ is made to transition to another trajectory, the remaining part of τ may become less important.

This paper is organized as follows. Section 4 introduces the conditional decision diffuser with rewards (DDR), including DDR-I which generates full trajectories conditioned on high returns, and DDR-II which generates the reward given the current and next states. Based on these constructs, the TSKD algorithm is presented in Section 5, and its superior performance in knowledge distillation is empirically demonstrated in Section 6. The paper is primed with the preliminaries in Section 3.

TSKD is also illustrated in Figure 1. The offline dataset is first used to train a trajectory generator (DDR-I) and a reward generator (DDR-II). The trajectories from DDR-I are blended with the original dataset through a stitching algorithm, which progressively evaluates the candidate states to transition to by using a series of criteria, including the reward produced by DDR-II. The resulting pool is filtered based on the full trajectory return, and the remaining trajectories are utilized to train a shallow policy via BC.

2. Related Work

Knowledge distillation (Hinton et al., 2015) is a framework for transferring knowledge from one model, which is the teacher, to another model, which is the student. The knowledge distillation has been implemented in RL in recent works. A method was proposed to distill multiple task-specific policies into a single policy which is more parameter-efficient (Czarnecki et al., 2019). The DPD method (Lai et al., 2020) utilized two policies that interact with the same environment with different initializations to explore different perspectives of the environment and extract knowledge from each other to enhance their learning. The M&M method (Czarnecki et al., 2018) combined curriculum learning as well as distillation to allow agents to perform well in an environment with large action space.

A relatively new approach based on knowledge distillation using Decision Transformer was introduced to solve offline multi-agent RL problems (Tseng et al., 2022). Levine & Feizi (2023) proposed distilling in goal-conditioned Q-learning by minimizing the difference between the current Q-value function and the target Q-value function. Laskin et al. (2022) used knowledge distillation in RL to distill policy knowledge from an online RL algorithm to an autoregressive transformer.

Wang et al. (2023a) recently proposed augmenting BC using a diffusion model. However, the diffusion model there does not provide planning for the agent and does not include the high-return condition information. As a result, the diffusion model does not represent a well-learned policy while ours does. Moreover, the BC training in their model intertwines with updates of the diffusion model, while we separate them into two stages with improved efficiency and simplicity.

3. Preliminary

We follow the standard setting of Markov decision process (MDP), which is defined by the tuple $\langle \rho_0, \mathcal{S}, \mathcal{A}, \mathcal{T}, \mathcal{R}, \gamma \rangle$. Here ρ_0 is the initial distribution. \mathcal{S} is the m -dimensional state space, and \mathcal{A} is the action space. $\mathcal{T} : \mathcal{S} \times \mathcal{A} \rightarrow \Delta_{\mathcal{S}}$ is the transition function. $\mathcal{R} : \mathcal{S} \times \mathcal{A} \times \mathcal{S} \rightarrow \mathbb{R}$ is the reward function. $\gamma \in [0, 1)$ is a discount factor (Puterman, 1995). The agent in this environment acts with a policy $\pi : \mathcal{S} \rightarrow \mathcal{A}$, generating a sequence of state-action-reward transitions, which represents a trajectory $\tau := (s_t, a_t, r_t)_{t \geq 0}$ with probability $p_{\pi}(\tau)$. The return of the trajectory is defined as $R(\tau) := \sum_{t \geq 0} \gamma^t r_t$.

Behavioural Cloning A BC agent learns a policy $\pi(a|s)$ by performing supervised learning on the dataset sampled from the environment $\mathcal{D} = \{(s_t, a_t, r_t, s'_t)\}$. Here, s'_t denotes the next state for the transition. BC seeks the optimal policy π_{θ} parameterized with θ by minimizing the risk

$$\mathcal{L}_{BC} := \mathbb{E}_{s, a \sim \mathcal{D}} [(\pi_{\theta}(s) - a)^2].$$

Extension to stochastic policy is straightforward, and we just keep the exposition simple because our work focuses on augmenting the offline dataset that is used for BC training.

BC can be implemented easily by parameterizing the policy with a Multilayer Perceptron (MLP), using a relatively small amount of parameters. However, BC performs poorly when the quality of the transitions in the dataset is not high. Therefore, in this work we aim to perform knowledge distilling from a deep generative model of the trajectories, which in our case is a decision diffuser with reward, to extract high-return trajectories to augment the dataset through a nontrivial stitching process. As a result, the policy learned from BC can be both effective and simple, representing an efficacious distillation from the deep generative model.

Diffusion Probabilistic Models Diffusion models (Ho et al., 2020) are a class of generative models that learn the data distribution $q(\mathbf{x})$ from a dataset $\mathcal{D} := \{\mathbf{x}^i\}_{0 \leq i < M}$. One of the major usage of these models is generating high-quality images from text descriptions (Saharia et al., 2022). The diffusion models consist of two processes, which are the forward process and the reverse process. For the forward process, the model will add noise step by step via a predefined way $q(\mathbf{x}_{k+1}|\mathbf{x}_k) := \mathcal{N}(\mathbf{x}_{k+1}; \sqrt{\alpha_k}\mathbf{x}, (1 - \alpha_k)\mathbf{I})$. For the reverse process, the model has trainable parameters in order to learn a good way to denoise step by step, which can be represented mathematically as $p_{\theta}(\mathbf{x}_{k-1}|\mathbf{x}_k) := \mathcal{N}(\mathbf{x}_{k-1}|\mu_{\theta}(\mathbf{x}_k, k), \Sigma_k)$. In these processes, $\mathcal{N}(\mu, \Sigma)$ denotes a Gaussian distribution with mean μ and covariance matrix Σ , and $\alpha_k \in \mathbb{R}$ determines the variance schedule. $\mathbf{x}_0 := \mathbf{x}$ denotes the original sample, while $\mathbf{x}_1, \mathbf{x}_2, \dots, \mathbf{x}_{K-1}$ are the middle steps for the diffusion, and $\mathbf{x}_K \sim \mathcal{N}(\mathbf{0}, \mathbf{I})$ is the pure Gaussian noise.

As for the trainable reverse process, it has a simplified loss function (Ho et al., 2020)

$$\mathcal{L}_{denoise}(\theta) := \mathbb{E}_{k \sim [1, K], \mathbf{x}_0 \sim q, \epsilon \sim \mathcal{N}(\mathbf{0}, \mathbf{I})} [\|\epsilon - \epsilon_{\theta}(\mathbf{x}_k, k)\|^2].$$

The model of predicting the noise $\epsilon_{\theta}(\mathbf{x}_k, k)$ is parameterized by a deep temporal U-Net (Janner et al., 2022). This is equivalent to modeling the mean of $p_{\theta}(\mathbf{x}_{k-1}|\mathbf{x}_k)$ as $\mu_{\theta}(x_{k-1}|x_k)$ can be calculated from $\epsilon_{\theta}(\mathbf{x}_k, k)$ (Ho et al., 2020).

Guided Diffusion The diffusion training process can be guided using conditional data. In order to avoid the need of a strong classifier, classifier-free guidance method (Ho & Salimans, 2022) is preferred. This method learns both a conditional model $\epsilon_{\theta}(\mathbf{x}_k, \mathbf{y}, k)$ and an unconditional model $\epsilon_{\theta}(\mathbf{x}_k, \emptyset, k)$, where \mathbf{y} is the label and \emptyset is a dummy value that takes the place of \mathbf{y} for unconditional situations. The perturbed noise can be denoted as $\epsilon_{\theta}(\mathbf{x}_k, \emptyset, k) + \omega(\epsilon_{\theta}(\mathbf{x}_k, \mathbf{y}, k) - \epsilon_{\theta}(\mathbf{x}_k, \emptyset, k))$, where ω denotes the guidance scale or the trade-off factor.

Knowledge Distillation Knowledge distillation (KD) transfers knowledge from one deep learning model (the teacher) to another (the student). It was originally proposed by minimizing the KL divergence of the outputs between the teacher model and the student model (Hinton et al., 2015).

Our work proposes a distillation framework that transfers the knowledge of a well-learned policy based on deep generative models to a relatively shallow model such as BC network by augmenting the dataset via trajectory stitching.

4. Decision Diffuser with Rewards

We first present our teacher model Decision Diffuser with Rewards (DDR), and its knowledge will be distilled. Decision Diffuser (DD, Ajay et al., 2023) is able to generate state-action pairs (s_t, a_t) with a *conditional* diffusion model and an inverse dynamics model (IDM). In real applications, most environments do not employ a predefined reward function. Therefore, given any offline RL algorithm that learns from an offline dataset with rewards $\mathcal{D} = \{(s_t, a_t, r_t, s'_t)\}$, any data augmentation approach should be able to generate full trajectories that includes rewards. Therefore, compared with the original Decision Diffuser, our model is able to generate not only states and actions but also rewards. Compared with knowledge distillation methods of goal-conditioned Q -learning (Levine & Feizi, 2023), our DDR model does not require estimating any kind of Q -function.

Analogously to Ajay et al. (2023), we only model the sequence of state and reward by a diffusion model. The sequence over actions, which are often represented as joint torques, tend to have higher frequency and are less smooth, making them much harder to model (Tedrake, 2022). We therefore decide to diffuse only on the states and rewards.

Although it appears trivial to extend the state-based diffuser to include rewards, our subsequent stitching algorithm raises an extra question that demands nontrivial modeling:

Given the current state s and a *candidate* next state \hat{s}' , how much would the reward r be?

This will impact the decision of stitching/transitioning from trajectory τ_A (where s lies) to τ_B (where \hat{s}' lies). In this case, it is necessary to model the reward based on both the current state and the next state. Otherwise, the model will only predict the next reward in the trajectory τ_A while disregarding the information from τ_B , possibly leading to biased reward prediction for the stitching transition.

So we develop two models for reward conditional diffusion:

- **DDR-I**: a diffuser that directly generates full trajectories. The reward only needs to depend on the most recent history of states.
- **DDR-II**: a diffuser that generates reward depending on the current state *and* the next proposed state, without action.

It may appear cumbersome to train two diffusers. In particular, since DDR-II models $(s_t, s_{t+1}, r_t, s_{t+1}, s_{t+2}, r_{t+1})$ sequences as in (4), it could also be used to generate the full trajectory which only requires modeling $(s_t, r_t, s_{t+1}, r_{t+1})$ sequences as in (3). However, the dimensionality of the former diffusion variables is about a half higher than that of the latter, which may introduce difficulty for the former diffuser to predict both the reward and the next state. So we would rather make more efficient use of the samples by training a separate but smaller model for the next state prediction while only leaving the reward prediction task for the larger model.

4.1. Conditional Diffusion Models for Decision Making

We can formulate sequential decision-making as the standard problem of conditional generative modeling:

$$\max_{\theta} \mathbb{E}_{\tau \sim \mathcal{D}} [\log p_{\theta}(\mathbf{x}_0(\tau) | \mathbf{y}(\tau))]. \quad (1)$$

Our aim is to generate partial trajectory $\mathbf{x}_0(\tau)$ using the information of conditioning data $\mathbf{y}(\tau)$. The conditioning data can be the return of the trajectory, the constraints satisfied by the trajectory, or the skill demonstrated in the trajectory. In our problem, we intend to generate high return trajectories with good policy. As such, we will use the return $R(\tau)$ as our conditioning data $\mathbf{y}(\tau)$.

We can then construct our generative model according to the conditional diffusion process:

$$q(\mathbf{x}_{k+1}(\tau) | \mathbf{x}_k(\tau)), \quad p_{\theta}(\mathbf{x}_{k-1}(\tau) | \mathbf{x}_k(\tau), \mathbf{y}(\tau)). \quad (2)$$

Here, q represents the forward diffusion process while p_{θ} represents the trainable reverse process parameterized by θ .

Algorithm 1 DDR-I for Trajectory Generation

- 1: **Input:** Noise model ϵ_{θ} , inverse dynamics f_{ϕ} , guidance scale ω , history length C , condition \mathbf{y}
 - 2: **Initialize** $h \leftarrow \text{Queue}(\text{length} = C)$
 - 3: Initialize an empty trajectory τ
 - 4: **for** $t = 0, 1, \dots$ until done **do**
 - 5: Observe state s and $h.\text{insert}(s)$. Set $s_t \leftarrow s$.
 - 6: Initialize $\mathbf{x}_K(\tau) \sim \mathcal{N}(\mathbf{0}, \alpha \mathbf{I})$ in $\mathbb{R}^{H(m+1)}$ from (3)
 - 7: **for** $k = K \dots 1$ **do**
 - 8: $\mathbf{x}_k(\tau)[:\text{length}(h)].\text{states} \leftarrow h$
 - 9: Set $\hat{\epsilon}$ with Equation 5, using θ , $\mathbf{x}_k(\tau)$, \mathbf{y} , and k
 - 10: $(\mu_{k-1}, \Sigma_{k-1}) \leftarrow \text{Denoise}(\mathbf{x}_k(\tau), \hat{\epsilon})$
 - 11: $\mathbf{x}_{k-1}(\tau) \sim \mathcal{N}(\mu_{k-1}, \alpha \Sigma_{k-1})$
 - 12: **end for**
 - 13: $r_t \leftarrow \mathbf{x}_0(\tau)[C-1].\text{reward}$, and $s_{t+1} \leftarrow \mathbf{x}_0(\tau)[C].\text{state}$
 - 14: Execute $a_t = f_{\phi}(s_t, s_{t+1})$ from IDM
 - 15: $\tau.\text{append}((s_t, a_t, r_t, s_{t+1}))$
 - 16: **end for**
-

Compared with the original Diffusion Probabilistic Model (Ho et al., 2020), the reverse process here has an additional conditioning label $\mathbf{y}(\tau)$, which in our case is the return of the trajectory, guiding the reverse process with high return condition and enabling the model to learn a good policy in the environment.

4.2. DDR-I for Trajectory Generation

We will apply the diffusion model in an auto-regression fashion to generate a trajectory. To this end, we diffuse over the following state for diffusion timesteps $k = 1, \dots, K$:

$$\mathbf{x}_k(\tau) := (s_{t-C+1}, r_{t-C+1}, \dots, s_t, r_t, \dots, s_{t+H-C}, r_{t+H-C})_k. \quad (3)$$

Here, t denotes the index in a trajectory in the offline RL dataset. We will refer to the entry of s_{t-C+1} as $\mathbf{x}_k(\tau)[0].\text{state}$, and the entry of r_{t-C+1} as $\mathbf{x}_k(\tau)[0].\text{reward}$. In the process of diffusion, it is crucial to make the current part of the trajectory consistent with the history. Therefore, we introduce the most recent C number of states by repeatedly overwriting the entries of s_{t-C+1}, \dots, s_t in $\mathbf{x}_k(\tau)$, throughout all diffusion steps k . We finally extract r_t and s_{t+1} from $\mathbf{x}_0(\tau)$. The whole generation procedure is formalized in Algorithm 1 and is illustrated in Figure 2.

It is noteworthy that we do not write in the reward from the latest C steps, differing from the states. Instead, we just let the diffuser fill in their values, which is consistent with our postulation that past states provide sufficient information to predict the reward. Further, although we do not pursue it in this work, DDR-I could also be used in online model-based planning, in which case the past rewards may not be even available to the agent online.

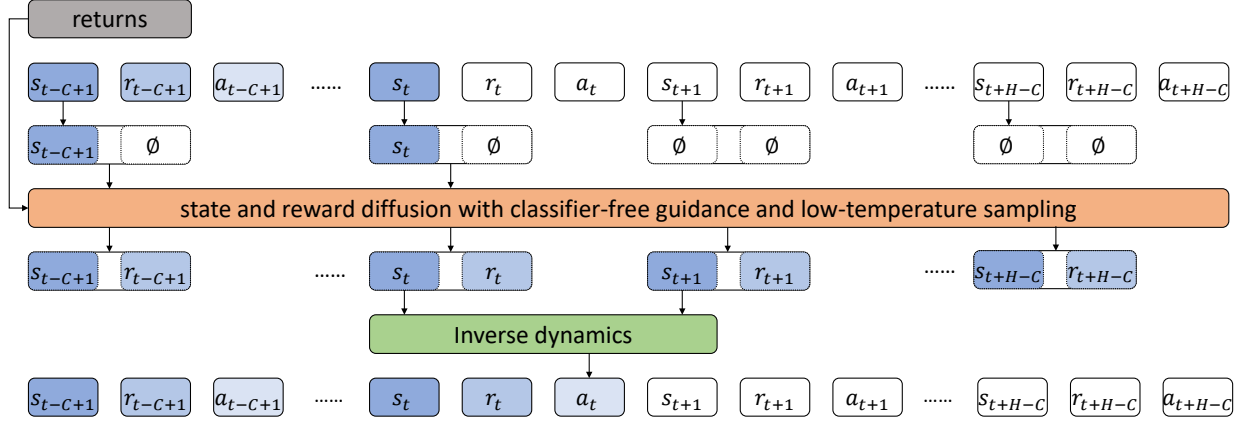


Figure 2. The trajectory generation phase for the model DDR-I. Given the latest C number of states s_{t-C+1}, \dots, s_t , the diffuser uses classifier-free guidance with low-temperature sampling to generate a sequence of future states and rewards. IDM is applied to generate action a_t with s_t and s_{t+1} . \emptyset means the value is left for the diffuser to fill in, instead of clamping with the observation (if available).

Algorithm 2 DDR-II for Reward Generation

- 1: **Input:** Noise model ϵ_θ , guidance scale ω , condition \mathbf{y} , current state s , stitching candidate s'
- 2: Initialize $\mathbf{x}_K(\tau) \sim \mathcal{N}(\mathbf{0}, \alpha \mathbf{I})$ in $\mathbb{R}^{H(2m+1)}$ from (4)
- 3: **for** $k = K \dots 1$ **do**
- 4: $\mathbf{x}_k(\tau)[0].\text{states} \leftarrow (s, s')$
- 5: Set $\hat{\epsilon}$ with Equation 5, using θ , $\mathbf{x}_k(\tau)$, \mathbf{y} , and k
- 6: $(\mu_{k-1}, \Sigma_{k-1}) \leftarrow \text{Denoise}(\mathbf{x}_k(\tau), \hat{\epsilon})$
- 7: $\mathbf{x}_{k-1}(\tau) \sim \mathcal{N}(\mu_{k-1}, \alpha \Sigma_{k-1})$
- 8: **end for**
- 9: **Return:** $\mathbf{x}_0(\tau)[0].\text{reward}$, i.e., the r_t in (4)

4.3. DDR-II for Reward Generation

DDR-II aims to generate the reward r_t given the current state s_t and the next state s_{t+1} . To apply a diffuser, define

$$\mathbf{x}_k(\tau) := (s_t, s_{t+1}, r_t, s_{t+1}, s_{t+2}, r_{t+1}, \dots, s_{t+H-1}, s_{t+H}, r_{t+H-1})_k, \quad 1 \leq k \leq K. \quad (4)$$

During the diffusion process, we introduce the given s_t and s_{t+1} by clamping the first two entries of $\mathbf{x}_k(\tau)$ for all diffusion steps k . We do not enforce that the generated fourth entry must be equal to the second one as in (4), although, of course, they are equal at training phase. It is also possible to take into account the state of the past C number of steps, akin to DDR-I. However, in practice we noticed that this does not provide much improvement, suggesting that s_t and s_{t+1} are sufficient to predict r_t . Algorithm 2 details the generation of reward by DDR-II.

4.4. Conditioning with Classifier-free Guidance

Both DDR-I and DDR-II employ classifier-free guidance to integrate conditional influence into the diffusion process. This is superior to using a classifier that requires estimating the Q -function (Ajay et al., 2023). We adopt the approach

of classifier-free guidance (Ho & Salimans, 2022), which defines the perturbed noise as

$$\hat{\epsilon} := \epsilon_\theta(\mathbf{x}_k(\tau), \emptyset, k) + \omega \cdot [\epsilon_\theta(\mathbf{x}_k(\tau), \mathbf{y}(\tau), k) - \epsilon_\theta(\mathbf{x}_k(\tau), \emptyset, k)], \quad (5)$$

where the scalar ω tends to augment and extract the best portions of trajectories in the dataset that comply with the conditioning of $\mathbf{y}(\tau)$, i.e., high return here. This helps the decision diffuser to learn a good policy from an average dataset. In the trajectory stitching part of our method, we will seek to transfer the information of this good policy into a smaller network such as the BC policy.

Training scheme Both DDR-I and DDR-II are trained in a supervised manner, using a dataset \mathcal{D} with trajectories sampled from the environment. Each batch of states are labeled with the returns they achieve via $R(s_t) = \sum_{i=t}^{t+H} \gamma^{i-t} r_i$. DDR-I and DDR-II are trained separately where the reverse diffusion process p_θ is parameterized by a noise model ϵ_θ :

$$\mathcal{L}_{DDR}(\theta) := \mathbb{E}_{\epsilon, k, \tau \in \mathcal{D}, \beta \sim \text{Bern}(p)} [\|\epsilon - \epsilon_\theta(\mathbf{x}_k(\tau), (1-\beta)\mathbf{y}(\tau) + \beta\emptyset, k)\|^2]. \quad (6)$$

For each trajectory τ , we first sample a noise $\epsilon \sim \mathcal{N}(\mathbf{0}, \mathbf{I})$ and a timestep $k \sim \mathcal{U}\{1, \dots, K\}$. Then, we construct the noisy array of $\mathbf{x}_k(\tau)$ that combines states and rewards in the manners of DDR-I and DDR-II. The DDR models are trained so that the noise can be well predicted by $\hat{\epsilon}_\theta := \epsilon_\theta(\mathbf{x}_k(\tau), \mathbf{y}(\tau), k)$.

4.5. Inverse Dynamics Model

Sampling states and rewards using a diffusion model is not enough for generating a full trajectory or extracting policy. A policy can be inferred from estimating the action a_t that leads the state s_t to s_{t+1} at any time index t in the

Algorithm 3 Trajectory Stitching for Knowledge Distilling in an abbreviated form. A detailed version is in Algorithm 4.

```

1: Input: a dataset  $\mathcal{D}_0$  with  $T$  trajectories  $(\tau_1, \dots, \tau_T)$ 
2: for  $k = 0, \dots, K$  do
3:   Generate  $n$  trajectories  $\mathcal{D}'_k$  using DDR-I
4:    $\mathcal{D}_k \leftarrow \text{concat}(\mathcal{D}_k, \mathcal{D}'_k)$ 
5:   Train the state-value function  $V$  on dataset  $\mathcal{D}_k$ .
6:   for  $t = 1, \dots, T$  (i.e., length of  $\mathcal{D}_k$ ) do
7:      $(s, s') \leftarrow (s_0, s'_0)$  from  $\tau_t$ . Initialize a new traj  $\hat{\tau}_t$ 
8:     while not done do
9:       if a state  $\hat{s}'$  in  $\mathcal{D}_k$  (possibly in a different trajectory than  $t$ ) is good to stitch to then
10:        Generate action  $\tilde{a}$  based on  $(s, \hat{s}')$  by IDM
11:        Generate reward  $\tilde{r}$  given  $(s, \hat{s}', \tilde{a})$  by DDR-II
12:        Add  $(s, \tilde{a}, \tilde{r}, \hat{s}')$  to the new trajectory  $\hat{\tau}_t$ 
13:         $s \leftarrow \hat{s}'$ 
14:         $s' \leftarrow$  the next state on the trajectory of  $\hat{s}'$ 
15:       else
16:        Add original transition to  $\hat{\tau}_t$  and slide  $(s, s')$ 
17:       end if
18:     end while
19:   end for
20:    $\mathcal{D}_{k+1} \leftarrow T$  trajectories in  $\{\hat{\tau}_t\}$  with the highest return
21: end for
22: Return: dataset  $\mathcal{D}_{K+1}$  for behavioural cloning training
    
```

trajectory τ . The Model-based Trajectory Stitching method (MBTS, Hepburn & Montana, 2023) proposed implementing the IDM $p(a_t|s_t, s_{t+1})$ with a conditional variational autoencoder. However, they are generally harder to train with a more complicated structure than MLPs. Therefore, we adopt the IDM from Pathak et al. (2018) that is also used by the Decision Diffuser (Ajay et al., 2023). In particular, $a_t := f_\phi(s_t, s_{t+1})$, where f_ϕ is an MLP with parameter ϕ . The training objective of IDM is simply

$$\mathcal{L}_{IDM}(\phi) := \mathbb{E}_{(s,a,s') \in \mathcal{D}} [\|a - f_\phi(s, s')\|^2]. \quad (7)$$

Ajay et al. (2023) showed that using IDMs is more effective than jointly diffusing over actions and states.

5. Trajectory Stitching Knowledge Distilling

MBTS (Hepburn & Montana, 2023) augments the dataset \mathcal{D} by stitching together high-value regions of different trajectories. The candidate states for stitching are determined by the state-value function $V(s)$ and the forward dynamics probability $p(s'|s)$. The stitching method is able to modify the original dataset \mathcal{D} and create higher-return trajectories by introducing new transitions between two states on the different trajectories, improving the result of BC. However, MBTS does not generate new trajectories conditioned with high return, leaving the stitched data still sub-optimal.

To address this issue, we propose the Trajectory Stitching

Knowledge Distilling (TSKD) method in Algorithm 3 (an abridged version), and it is compared with MBTS which is formalized in Algorithm 5 (Appendix A). The key differences are highlighted in color. The detailed TSKD method is deferred to Algorithm 4 in Appendix A, and the overall process is illustrated in Figure 1. It leverages DDRs to generate trajectories conditioned on high returns, and stitches with original trajectories to avoid overfitting high-return regimes by also covering other areas. Training on these TSKD-empowered trajectories by BC allows the DDR models’ knowledge to be transferred to the learned policy, retaining similar performance to the deep models while significantly distilling them into a much shallower MLP. In this case, the DDR models are the teacher and the BC policy model is the student for knowledge distillation.

The key step of Algorithm 3 is step 9, where a candidate state \hat{s}' is evaluated for stitching. By “good”, we follow MBTS to demand three conditions as detailed in Algorithm 4. Firstly, it needs to be close to s' , and we detail the neighborhood selection in Appendix B.1. Secondly, there is a good chance to switch to \hat{s}' . To be self-contained, we recap the criterion from MBTS in Section 5.1. Thirdly, the value of \hat{s}' is higher than s' , which we discuss in Section 5.2.

5.1. Forward Dynamics Criterion

To determine whether a state can be a candidate next state for stitching, we need a criterion based on forward dynamics model $p(s'|s)$, depicting the transition probability from state s to the possible candidate state s' , which may differ from the observed next state s' . We model the environment dynamics as a Gaussian distribution, which is common for continuous state-space applications (Janner et al., 2019). We create an ensemble \mathcal{E} of N dynamics models parameterized by ξ^i : $\{\hat{p}_{\xi^i}(s_{t+1}|s_t) = \mathcal{N}(\mu_{\xi^i}(s_t), \Sigma_{\xi^i}(s_t))\}_{i=1}^N$. Each model is trained via maximum likelihood estimation from the dataset \mathcal{D} , for which the loss can be formulated as:

$$\mathcal{L}_{\hat{p}}(\xi) := \mathbb{E}_{s,s' \sim \mathcal{D}} [(\mu_\xi(s) - s')^T \Sigma_\xi^{-1}(s) (\mu_\xi(s) - s') + \log |\Sigma_\xi(s)|], \quad (8)$$

where $|\cdot|$ is the determinant of a matrix. We train the ensemble using different parameter initializations for each model in order to take the epistemic uncertainty into account.

We formulate the criterion for determining the candidate next state in a conservative manner:

$$\min_{i \in \mathcal{E}} \hat{p}_{\xi^i}(s'|s) > \text{mean}_{i \in \mathcal{E}} \hat{p}_{\xi^i}(s'|s). \quad (9)$$

5.2. Value Function Criterion

In order to measure if a state is worth stitching, a common approach trains a value function over the dataset \mathcal{D} . As the states on the DDR-generated trajectories tend to have a high

Table 1. **Normalized average score on D4RL datasets.** We show that our knowledge distillation method (DDR+TSKD+BC) matches or outperforms the state-of-the-art offline RL algorithms, while only using a shallow BC network as the student model that distills a deep DDR model (the teacher model). In particular, our method outperforms the original trajectory stitching method (MBTS+BC). We report the mean and the standard error over 5 random seeds. We highlight in **lime** when an algorithm’s average performance in a given category is at most 5% below the optimal, and in **boldface** if the performance for an individual environment is at most 7% below the optimal.

	ALGORITHMS →	BC	CQL	IQL	DT	TT	DP	DD	MBTS+BC	DDR+TSKD+BC
# PARAMETERS	(IN MILLIONS) →	0.07	-	-	0.86	1.39	2.18	59.73	0.07	0.07
DATASET	ENVIRONMENT									
MED-EXPERT	HALFCHEETAH	55.2	91.6	86.7	86.8	95	79.8	90.6	86.9	86.8±0.7
MED-EXPERT	HOPPER	52.5	105.4	91.5	107.6	110.0	107.2	111.8	94.8	105.1±6.1
MED-EXPERT	WALKER2D	107.5	108.8	109.6	108.1	101.9	108.4	108.8	108.8	109.1±0.1
AVERAGE	-	71.7	101.9	95.9	100.8	102.3	98.4	103.7	96.8	100.3±2.3
MEDIUM	HALFCHEETAH	42.6	44.0	47.4	42.6	46.9	44.2	49.1	43.2	44.1±0.7
MEDIUM	HOPPER	52.9	58.5	66.3	67.6	61.1	58.5	79.3	64.3	83.2±8.1
MEDIUM	WALKER2D	75.3	72.5	78.3	74.0	79	79.7	82.5	78.8	78.5±2.0
AVERAGE	-	56.9	58.3	64	61.4	62.3	60.8	70.3	62.1	68.6±3.6
MED-REPLAY	HALFCHEETAH	36.6	45.5	44.2	36.6	41.9	42.2	39.3	39.8	38.9±3.2
MED-REPLAY	HOPPER	18.1	95	94.7	82.7	91.5	96.8	100	50.2	96.4±6.8
MED-REPLAY	WALKER2D	26.0	77.2	73.9	66.6	82.6	61.2	75	61.5	74.5±6.5
AVERAGE	-	26.9	72.6	70.9	62.0	72.0	66.7	71.4	50.5	69.9±5.5
MIXED	KITCHEN	51.5	52.4	51	-	-	-	65	-	60.0±4.8
PARTIAL	KITCHEN	38	50.1	46.3	-	-	-	57	-	44.4±3.9
AVERAGE	-	44.8	51.2	48.7	-	-	-	61	-	52.2±4.4

value, they enjoy a higher chance of stitching, hence promoting these states to be blended into the original dataset.

We approximate the value function using an MLP with parameter β . The Bellman error is minimized on dataset \mathcal{D} :

$$\mathcal{L}_V(\beta) := \mathbb{E}_{s,r,s' \sim \mathcal{D}}[(r + \gamma V_\beta(s') - V_\beta(s))^2]. \quad (10)$$

Since V_β is applied only to in-distribution states, it avoids the out-of-distribution issue when evaluating value function.

6. Experiments

We now demonstrate the empirical performance of TSKD for offline RL. We emphasize that our goal is knowledge distillation – instead of only comparing the performance, we aim to retain or improve upon the performance of the state of the art by using a much smaller neural network. Note that our entire method is indeed DDR+TSKD+BC, but we just refer to it as TSKD for brevity when no ambiguity arises.

Environments We evaluated TSKD on standard locomotion tasks from the D4RL benchmark (Fu et al., 2020), including Halfcheetah, Hopper and Walker2d. To explore its robustness, we also tested on Kitchen, a harder task. We only considered the medium-expert, medium, and medium-replay datasets, because the BC model already performs nearly as well as the deep models in the expert datasets.

Baselines We compared TSKD with typical model-free methods for offline RL, such as CQL and IQL. We also adopted approaches based on large generative models, including trajectory transformer (TT), decision transformer (DT), decision diffuser (DD), and diffusion planner (DP, Janer et al., 2022). Moreover, we compared with MBTS+BC.

Settings We evaluated the performance using the *normalized average return* (Fu et al., 2020). It first applies the offline learned policy to 10 online episodes. The total reward of each episode is referred to as a *score*, which is then normalized via $100 \times \frac{\text{score} - \text{random score}}{\text{expert score} - \text{random score}}$. The process is repeated with 5 random seeds, producing mean and variance. TSKD used 300 trajectories generated from DDR-I. The detailed hyperparameter settings are relegated to Appendix B.

Policy model size The standard algorithms such as BC, CQL, and IQL do not need large models to achieve their best performance. TSKD augments the offline data by training large models. But the final policy is still learned via BC, which only uses a small model (70k parameters). MBTS adopts small models for both stitching and BC (70k). DT and TT do use moderately large transformers (1 million), while DP employs even larger diffusion models (2 million). The DD model, which often performs the best, is the largest, with about 60 million parameters.

The model size varies *slightly* with the environment/dataset,

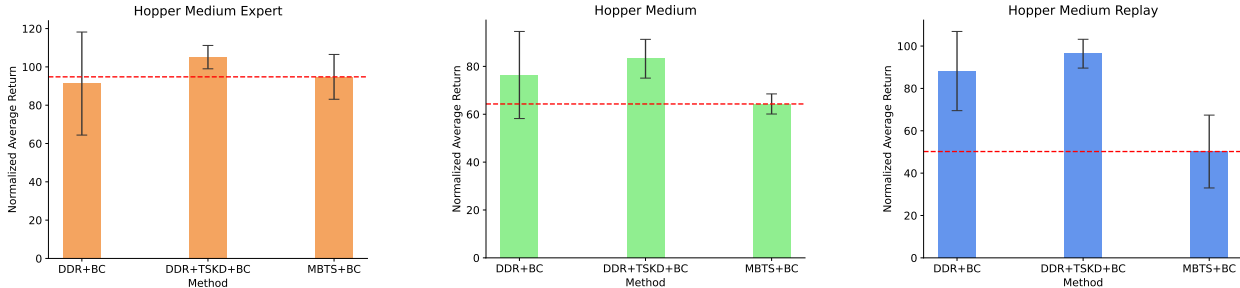


Figure 3. Ablation study on trajectory generation and stitching. We demonstrate the contribution of the two major components of DDR+TSKD+BC by comparing its performance against two variants: DDR+BC (dropping the stitching step) and MBTS+BC (besides DDR-I, this variant also drops DDR-II and some other modifications which are required by TSKD stitching. So we use MBTS+BC as an approximation.) The environment is Hopper, with three difficulty levels from left to right: medium expert, medium, and medium replay.

and we just report the average values. The competing methods were tuned to almost optimize their performance, while keeping their size as small as possible. Although additional hyperparameter tuning may further save the network size slightly, our policy model learned from TSKD is smaller by orders of magnitude, as shown in the second row of Table 1.

Performance results The results of normalized average score are shown in Table 1. Our TSKD generally matches or outperforms the deep generative models on the D4RL benchmark datasets. This is achieved by using only 70k parameters in our knowledge distilled student model during the planning phase. In contrast, the deep generative model based methods (DT, TT, DP, DD) employ a much larger number of parameters, resulting in high computational cost. We present more detailed comparisons on model size and time complexity in Appendix C.

Although the parameter size for model-free methods such as CQL and IQL is small, their sample efficiency is often lower, requiring a great amount of sampled data to learn well. In contrast, model-based methods, including our teacher DDR model, are able to leverage the offline data more efficiently.

We also observe that our TSKD outperforms MBTS in most cases, especially where expert knowledge is deficient. This corroborates the effectiveness of TSKD in extracting good policy knowledge from the deep generative models.

6.1. Ablation Study on the TSKD Method

Our first ablation study investigates how the two key ingredients of our method, namely DDR and TSKD, contribute to its performance. So we compared with two variants: a) only adding DDR-I generated trajectories to the datasets (DDR+BC), and b) only performing stitching without generating trajectories from DDR-I. However, the latter still requires DDR-II for stitching (line 12 of Algorithm 3) with some other modifications (details in Algorithm 4). Therefore, to completely remove DDR, we resort to MBTS+BC as an approximation of the ablated approach.

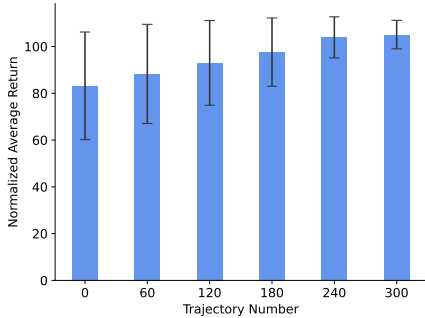


Figure 4. Ablation on the number of DDR-I generated trajectory. As we gradually reduce the number of generated trajectories from DDR-I that are fed into the trajectory stitching process, the performance degrades significantly. Data: Hopper medium expert.

The resulting normalized average score is compared in Figure 3 using the Hopper dataset with the same three difficulty levels as in Table 1. The results for Halfcheetah and Walker2d are deferred to Figure 6 in the appendix. Overall, DDR+BC is more effective than MBTS+BC, which indicates that the deep generative model is indeed helpful by providing high-return trajectories. Furthermore, DDR+TSKD+BC even outperforms DDR+BC, because the stitching step can avoid overfitting to the high-return regions by blending in transitions from the low value regions.

6.2. Ablation on the Number of Generated Trajectories

We next study the impact of the high-return trajectories generated by DDR-I. Figure 4 shows that, using Hopper medium expert as an example, the performance of our method can be improved with more trajectories sampled from DDR-I. Meanwhile, the variance also decays because a broader range of situations are fed to BC. When only a small number of high-return trajectories are available, some test episodes turned out to suffer a significantly lower score.

We finally analyzed the accuracy of DDR-II in generating reward, and the result is available in Appendix E.

Conclusions and future work We proposed a novel knowledge distilling method for offline RL, where two new large conditional diffusion models (DDR-I and DDR-II) are trained so that the sampled trajectories with a high return are blended with the original ones via a novel stitching method TSKD. This allows BC to learn a much smaller student model while retaining the good performance.

TSKD can be extended to multi-teacher distillation (You et al., 2017) by training a set of DDR models from different knowledge sources. Besides combining their generated trajectories, different DDR-II models can also improve TSKD by providing epistemic uncertainty on reward generation.

Impact Statement

This paper presents work whose goal is to advance the field of Machine Learning. There are many potential societal consequences of our work, none of which we feel must be specifically highlighted here.

References

- Ajay, A., Du, Y., Gupta, A., Tenenbaum, J., Jaakkola, T., and Agrawal, P. Is conditional generative modeling all you need for decision-making? In *International Conference on Learning Representations*, 2023.
- Castro, P. S. Scalable methods for computing state similarity in deterministic markov decision processes. In *Proceedings of the AAAI Conference on Artificial Intelligence*, 2020.
- Chen, L., Lu, K., Rajeswaran, A., Lee, K., Grover, A., Laskin, M., Abbeel, P., Srinivas, A., and Mordatch, I. Decision transformer: Reinforcement learning via sequence modeling. In *Advances in Neural Information Processing Systems*, 2021.
- Czarnecki, W. M., Jayakumar, S. M., Jaderberg, M., Hasenclever, L., Teh, Y. W., Osindero, S., Heess, N., and Pascanu, R. Mix & match - agent curricula for reinforcement learning. In *International Conference on Machine Learning*, 2018.
- Czarnecki, W. M., Pascanu, R., Osindero, S., Jayakumar, S. M., Swirszcz, G., and Jaderberg, M. Distilling policy distillation. In *The 22th International Conference on Artificial Intelligence and Statistics*, 2019.
- Fu, J., Kumar, A., Soh, M., and Levine, S. Diagnosing bottlenecks in deep q-learning algorithms. In *International Conference on Machine Learning (ICML)*, pp. 2021–2030, 2019.
- Fu, J., Kumar, A., Nachum, O., Tucker, G., and Levine, S. D4RL: datasets for deep data-driven reinforcement learning. *CoRR*, abs/2004.07219, 2020. URL <https://arxiv.org/abs/2004.07219>.
- Fujimoto, S., Meger, D., and Precup, D. Off-policy deep reinforcement learning without exploration. In *International Conference on Machine Learning (ICML)*, 2019.
- Hepburn, C. A. and Montana, G. Model-based trajectory stitching for improved behavioural cloning and its applications. *Machine Learning*, 2023.
- Hinton, G., Vinyals, O., and Dean, J. Distilling the knowledge in a neural network. In *arXiv preprint arXiv:1503.02531*, 2015.

- Ho, J. and Salimans, T. Classifier-free diffusion guidance. In *arXiv preprint arXiv:2207.12598*, 2022.
- Ho, J., Jain, A., and Abbeel, P. Denoising diffusion probabilistic models. In *Advances in Neural Information Processing Systems*, 2020.
- Janner, M., Fu, J., Zhang, M., and Levine, S. When to trust your model: Model-based policy optimization. In *Advances in Neural Information Processing Systems*, 2019.
- Janner, M., Li, Q., and Levine, S. Offline reinforcement learning as one big sequence modeling problem. *CoRR*, abs/2106.02039, 2021a. URL <https://arxiv.org/abs/2106.02039>.
- Janner, M., Li, Q., and Levine, S. Offline reinforcement learning as one big sequence modeling problem. In *Advances in Neural Information Processing Systems*, 2021b.
- Janner, M., Du, Y., Tenenbaum, J., and Levine, S. Planning with diffusion for flexible behavior synthesis. In *International Conference on Machine Learning*, 2022.
- Kingma, D. P. and Ba, J. Adam: A method for stochastic optimization. In *International Conference for Learning Representations*, 2015.
- Kostrikov, I., Nair, A., and Levine, S. Offline reinforcement learning with implicit q-learning. *CoRR*, abs/2110.06169, 2021. URL <https://arxiv.org/abs/2110.06169>.
- Kumar, A., Fu, J., Soh, M., Tucker, G., and Levine, S. Stabilizing off-policy Q-learning via bootstrapping error reduction. In *Advances in Neural Information Processing Systems (NeurIPS)*, 2019.
- Kumar, A., Gupta, A., and Levine, S. Discor: Corrective feedback in reinforcement learning via distribution correction. In *Advances in Neural Information Processing Systems (NeurIPS)*, 2020a.
- Kumar, A., Zhou, A., Tucker, G., and Levine, S. Conservative Q-learning for offline reinforcement learning. In *Advances in Neural Information Processing Systems (NeurIPS)*, 2020b.
- Lai, K.-H., Zha, D., Li, Y., and Hu, X. Dual policy distillation. In *International Joint Conferences on Artificial Intelligence*, 2020.
- Langley, P. Crafting papers on machine learning. In Langley, P. (ed.), *Proceedings of the 17th International Conference on Machine Learning (ICML 2000)*, pp. 1207–1216, Stanford, CA, 2000. Morgan Kaufmann.
- Laskin, M., Wang, L., Oh, J., Parisotto, E., Spencer, S., Steigerwald, R., Strouse, D., Hansen, S., Filos, A., Brooks, E., Gazeau, M., Sahni, H., Singh, S., and Mnih, V. In-context reinforcement learning with algorithm distillation, 2022.
- Levine, A. and Feizi, S. Goal-conditioned q-learning as knowledge distillation. In *Proceedings of the AAAI Conference on Artificial Intelligence*, 2023.
- Levine, S., Kumar, A., Tucker, G., and Fu, J. Offline reinforcement learning: Tutorial, review, and perspectives on open problems. *arXiv preprint arXiv:2005.01643*, 2020.
- Luo, C. Understanding diffusion models: A unified perspective, 2022.
- Misra, D. Mish: A self regularized non-monotonic neural activation function. In *British Machine Vision Conference*, 2019.
- Nair, A., Gupta, A., Dalal, M., and Levine, S. AWAC: Accelerating online reinforcement learning with offline datasets. *arXiv preprint arXiv:2006.09359*, 2020.
- Pathak, D., Mahmoudieh, P., Luo, G., Agrawal, P., Chen, D., Shentu, Y., Shelhamer, E., Malik, J., Efros, A. A., and Darrell, T. Zero-shot visual imitation. In *Proceedings of the IEEE conference on computer vision and pattern recognition workshops*, 2018.
- Puterman, M. L. *Markov decision processes: discrete stochastic dynamic programming*. John Wiley & Sons, 1995.
- Saharia, C., Chan, W., Saxena, S., Li, L., Whang, J., Denton, E., Ghasemipour, S. K. S., Ayan, B. K., Mahdavi, S. S., and et al., R. G. L. Photorealistic text-to-image diffusion models with deep language understanding. In *arXiv preprint arXiv:2205.11487*, 2022.
- Tedrake, R. Underactuated robotics. In URL <http://underactuated.mit.edu>, 2022.
- Tseng, W.-C., Wang, T.-H. J., Lin, Y.-C., and Isola, P. Offline multi-agent reinforcement learning with knowledge distillation. In *Advances in Neural Information Processing Systems*, 2022.
- Wang, H.-C., Chen, S.-F., Hsu, M.-H., Lai, C.-M., and Sun, S.-H. Diffusion model-augmented behavioral cloning. In *arXiv preprint arXiv:2302.13335*, 2023a.
- Wang, Z., Hunt, J. J., and Zhou, M. Diffusion policies as an expressive policy class for offline reinforcement learning. In *International Conference on Learning Representations (ICLR)*, 2023b.

Wu, Y. and He, K. Group normalization. In *European Conference on Computer Vision*, 2018.

You, S., Xu, C., Xu, C., and Tao, D. Learning from multiple teacher networks. In *Proceedings of the 23rd ACM SIGKDD International Conference on Knowledge Discovery and Data Mining*, 2017.

A. Algorithm Details

We present the detailed pseudo-code for the Trajectory Stitching Knowledge Distilling (TSKD) in our method. Algorithm 4 also depicts the knowledge distilling process.

Algorithm 4 Trajectory Stitching Knowledge Distilling (detailed version)

Input: An inverse dynamics model f_ϕ , a DDR-I model D_θ^1 , a DDR-II model $D_{\theta'}^2$, an ensemble of dynamics models $\{\hat{p}_\xi^i(s_{t+1}|s_t)\}_{i=1}^N$, an acceptance threshold \tilde{p} , and a dataset \mathcal{D}_0 made up of T trajectories (τ_1, \dots, τ_T) , additional trajectory number n , sum of rewards threshold λ .

for $k = 0, \dots, K$ **do**

 Generate n new trajectories \mathcal{D}'_k using D_θ^1 model with Algorithm 1

$\mathcal{D}_k \leftarrow \text{concat}(\mathcal{D}_k, \mathcal{D}'_k)$

 Train state-value function V on dataset \mathcal{D}_k .

for $t = 1, \dots, \text{length}(\mathcal{D}_k)$ **do**

 Select $(s, s') = (s_0, s'_0)$ from τ_t

 Initialize new trajectory $\hat{\tau}_t$

while not done **do**

 Create a set of neighbourhood $\{\hat{s}_j\} = \mathcal{N}(s') \cap \{\text{states in } \mathcal{D}_k\}$

 Let $j = \arg \max_i V(\hat{s}'_i)$

if $\min_i \hat{p}_\xi^i(\hat{s}'_j|s) > \text{mean}_i \hat{p}_\xi^i(s'|s)$ and $V(\hat{s}'_j) > V(s')$ **then**

 Generate new action $\tilde{a} \sim f_\phi(s, \hat{s}'_j)$

 Generate new reward $\tilde{r} \sim D_{\theta'}^2(s, \hat{s}'_j)$ via Algorithm 2

 Add $(s, \tilde{a}, \tilde{r}, \hat{s}'_j)$ to new trajectory $\hat{\tau}_t$

 Set $s = \hat{s}'_j$, and s' to the next state on the trajectory of \hat{s}'_j

else

 Add original transition, (s, a, r, s') to the new trajectory $\hat{\tau}_t$

 Set $s = s'$, and s' to the next state on the trajectory of s

end if

end while

if $\sum_{i \in \hat{\tau}_t} r_i \leq (1 + \tilde{p}) \sum_{i \in \tau_t} r_i$ **then**

$\hat{\tau}_t = \tau_t$

end if

end for

 Sort the trajectories with the values of $\sum_{i \in \hat{\tau}_t} r_i$

$\mathcal{D}_{k+1} \leftarrow$ the top T trajectories from the sorting result

end for

$\mathcal{D}_{BC} \leftarrow$ Select the trajectories τ in the dataset \mathcal{D}_{k+1} satisfying $\sum_{i \in \tau} r_i > \lambda$

Train Behavioural Cloning on dataset \mathcal{D}_{BC}

We next recap, in Algorithm 5, the Model-based Trajectory Stitching (MBTS) method from (Hepburn & Montana, 2023).

Algorithm 5 Model-based Trajectory Stitching (MBTS)

```

1: Input: a dataset  $\mathcal{D}_0$  with  $T$  trajectories  $(\tau_1, \dots, \tau_T)$ 
2: for  $k = 0, \dots, K$  do
3:   Train the state-value function  $V$  on dataset  $\mathcal{D}_k$ .
4:   for  $t = 1, \dots, T$  (i.e., length of  $\mathcal{D}_k$ ) do
5:      $(s, s') \leftarrow (s_0, s'_0)$  from  $\tau_t$ .
6:     Initialize a new trajectory  $\hat{\tau}_t$ 
7:     while not done do
8:       if a state  $\hat{s}'$  in  $\mathcal{D}_k$  (possibly in a different trajectory than  $t$ ) is close to  $s'$  and is good to stitch to then
9:         Generate action  $\tilde{a}$  based on  $(s, \hat{s}')$  by IDM
10:        Generate reward  $\tilde{r}$  under  $(s, \hat{s}', \tilde{a})$  by WGAN
11:        Add  $(s, \tilde{a}, \tilde{r}, \hat{s}')$  to the new trajectory  $\hat{\tau}_t$ 
12:         $s \leftarrow \hat{s}'$ 
13:         $s' \leftarrow$  the next state on the trajectory of  $\hat{s}'$ 
14:       else
15:         Add original transition to  $\hat{\tau}_t$  and slide  $(s, s')$ 
16:       end if
17:     end while
18:   end for
19:    $\mathcal{D}_{k+1} \leftarrow (\hat{\tau}_1, \dots, \hat{\tau}_T)$   $\triangleright \mathcal{D}_k$  has constant length  $T$ 
20: end for
21: Return: dataset  $\mathcal{D}_{K+1}$  for Behavioural Cloning training

```

Our TSKD method differs from the MBTS method mainly in four aspects:

- Added extra generated trajectories for stitching via DDR-I.
- Used a deeper generative model (DDR-II) for reward generation.
- Used a different inverse dynamics architecture.
- Added filters to discard trajectories with low normalized average returns.

B. Hyperparameter and Architectural Details

In this section, we describe the hyperparameter choice for our model and the architectural details for our model:

- We use a temporal U-Net (Janner et al., 2022) for the noise ϵ_θ modeling. It consists a U-Net structure with 6 repeated residual blocks, while each block consisting two temporal convolutions, each followed by group norm (Wu & He, 2018), and a final Mish nonlinearity (Misra, 2019). Both of the timestep and condition embeddings are 128-dimensional vectors produced by two separate 2-layered MLP with 256 hidden units and Mish nonlinearity. The embeddings are concatenated together before getting added to the activations of the first temporal convolution within each block. Our code for the DDR model is a modification of the code for the original Decision Diffuser (Ajay et al., 2023), for which the link is <https://github.com/anuragajay/decision-diffuser>.
- We use a 2-layered MLP with 512 hidden units and ReLU activations for the modeling of the inverse dynamics model f_ϕ .
- We train ϵ_θ and f_ϕ using the Adam optimizer (Kingma & Ba, 2015) with a learning rate $2 \cdot 10^{-4}$ and batch size of 32 for $1e6$ training steps.
- We choose the probability p of removing the conditioning information to be 0.25.

- We use $K = 200$ diffusion steps.
- We choose context length $C \in \{1, 20\}$, $C = 20$ is preferred in the Kitchen datasets. Both C values are able to generate decent results in the locomotion datasets, but $C = 20$ tends to have more stability.
- We use a planning horizon H with $H - C = 100$ in all the D4RL locomotion tasks, while using $H - C = 56$ in D4RL kitchen tasks.
- We use a guidance scale $\omega \in \{1.2, 1.4, 1.6, 1.8\}$ but the exact choice varies by task.
- We choose $\alpha = 0.5$ for low temperature sampling.
- We use a 3-layered MLP with 300 hidden units with ReLU activation to model the forward dynamics. The network takes a state s for input and output a mean μ and a standard deviation σ for a Gaussian distribution $\mathcal{N}(\mu, \sigma^2)$. For all experiments, an ensemble size of 7 is used with the best 3 being chosen. We train the forward dynamics models with Adam optimizer (Kingma & Ba, 2015), a learning rate of $3 \cdot 10^{-4}$ and a batch size of 256. We initialize the parameter with different random seeds for each forward dynamics model in the ensemble.
- We choose to use a 2-layered MLP with 256 hidden units and a ReLU activation to parameterize the value function. We train two value functions with different parameter initialization and take the minimum of the two during the stitching process. We train the model with Adam optimizer and a learning rate of $3 \cdot 10^{-4}$ and a batch size of 256.
- We choose the neighbourhood radius $\rho \in \{0.1, 1.0, 3.0\}$ while the exact choice varies by task.
- We use the additional trajectory number $n = 300$ for each epoch during stitching.
- We use the sum of rewards threshold $\lambda = \max_t(\sum_{\tau_t} r^i) - \kappa$, while κ is in the range of $[500, 1000]$ depending on the task.
- We choose the acceptance threshold $\tilde{p} = 0.1$ to ensure the stitched trajectory only to be used when a significant improvement is guaranteed.
- We use a behavioural cloning model parameterized by a 2-layered MLP with 256 hidden units and ReLU activation.
- We choose to use the epoch number $K = 1, 2, 3, 4$. For most cases, using $K = 2$ will have the sufficient performance gain, and the results will saturate in the following epochs.

B.1. Neighborhood Selection

For trajectory stitching, we discourage stitching two states that are far away. In this case, stitching in a created neighbourhood for the next state is preferred. Multiple metrics are available to define the neighbourhood by measuring the distance in the state space. Castro (2020) proposed a pseudo-metric, but its computational cost is rather high. Therefore, we resort to a more straightforward approach by applying the L2 norm for neighbourhood selection:

$$\mathcal{N}(s) := \{\hat{s} : \|\hat{s} - s\|_2 < \rho\}, \tag{11}$$

where ρ is a hyperparameter with a relatively small value.

C. Planning Time Characteristics and Volume of Parameters

Online planning time is a crucial factor for offline RL algorithm deployment. With smaller amount of parameters and faster planning, the computational cost is lower and it's easier to achieve real-time decision planning. Using the Trajectory Stitching Knowledge Distilling method, we are able to transfer the policy knowledge from the Decision Diffuser with Rewards model and improve the performance of a Behavioural Cloning network to the level of matching or even outperforming the current deep neural methods. In this section we compare the time consumption during planning phase between our model and the Decision Diffuser model (Ajay et al., 2023). The results are shown in Table 2.

We compare the amount of parameters needed to be computed during the planning phase and the average performance over the D4RL locomotion datasets between our model and the Decision Diffuser (DD) (Ajay et al., 2023), the Decision

Table 2. Planning time characteristics comparison. Our method only consumes 0.88% of the time compares to the Decision Diffuser (DD) during planning phase, while producing nearly matching results. We evaluate the time consumption on 10 episodes for each method in the D4RL Hopper-Med-Expert dataset. We perform the comparison on a machine with a single RTX3080 graphic card with 10GB graphic memory. The time is in seconds.

-	200 STEPS	400 STEPS	600 STEPS	800 STEPS	1000 STEPS
DD	236.89±5.93	474.69±11.24	711.63±17.08	950.03±21.85	1185.19±23.83
DDR+TSKD+BC	2.08±0.02	4.16±0.03	6.24±0.05	8.32±0.07	10.40±0.09

Table 3. Planning parameters and performance analysis. We analyze the parameters needed to be computed during the planning phase of each model. The parameters are directly recorded from the model. The performance is the average on the D4RL locomotion datasets.

ENVIRONMENT	DD	DT	TT	DDR+TSKD+BC
HOPPER	59.73M	0.86M	1.23M	0.07M
HALFCHEETAH	59.74M	0.86M	1.47M	0.07M
WALKER2D	59.74M	0.86M	1.47M	0.07M
AVERAGE PERFORMANCE	81.8	74.7	78.9	79.6

Transformer (DT) (Chen et al., 2021) and the Trajectory Transformer (TT) (Janner et al., 2021a). The results are shown in Table 3.

We can observe that our method computes extremely quickly with extremely small amount of parameters during evaluation while achieving nearly matching results compares to the deep neural models. Therefore, it can benefit the deployment process in real-life environments with much smaller computational requirements.

D. Classifier-free Guidance Details

In this section, we show the derivation of the classifier-free guidance Eq.5 for completeness. From the derivation outlined in prior works (Luo, 2022), we know that $\nabla_{\mathbf{x}_k(\tau)} \log q(\mathbf{x}_k(\tau)|\mathbf{y}(\tau)) \propto -\epsilon_\theta(\mathbf{x}_k(\tau), \mathbf{y}(\tau), k)$. Furthermore, we can derive:

$$\begin{aligned}
 q(\mathbf{x}_k(\tau)|\mathbf{y}(\tau)) &= q(\mathbf{x}_k(\tau)) \frac{q(\mathbf{x}_k(\tau)|\mathbf{y}(\tau))}{q(\mathbf{x}_k(\tau))} \\
 \Rightarrow \log q(\mathbf{x}_k(\tau)|\mathbf{y}(\tau)) &= \log q(\mathbf{x}_k(\tau)) + (\log q(\mathbf{x}_k(\tau)|\mathbf{y}(\tau)) - \log q(\mathbf{x}_k(\tau)))
 \end{aligned}$$

In order to sample from $q(\mathbf{x}_0(\tau)|\mathbf{y}(\tau))$ with classifier-free guidance, we multiply the second term with conditional guidance factor ω :

$$\begin{aligned}
 \log \hat{q} &:= \log q(\mathbf{x}_k(\tau)) + \omega(\log q(\mathbf{x}_k(\tau)|\mathbf{y}(\tau)) - \log q(\mathbf{x}_k(\tau))) \\
 \Rightarrow \nabla_{\mathbf{x}_k(\tau)} \log \hat{q} &= \nabla_{\mathbf{x}_k(\tau)} \log q(\mathbf{x}_k(\tau)) + \omega(\nabla_{\mathbf{x}_k(\tau)} \log q(\mathbf{x}_k(\tau)|\mathbf{y}(\tau)) - \nabla_{\mathbf{x}_k(\tau)} \log q(\mathbf{x}_k(\tau))) \\
 \Rightarrow \hat{\epsilon} &:= \epsilon_\theta(\mathbf{x}_k(\tau), \emptyset, k) + \omega(\epsilon_\theta(\mathbf{x}_k(\tau), \mathbf{y}(\tau), k) - \epsilon_\theta(\mathbf{x}_k(\tau), \emptyset, k))
 \end{aligned}$$

In this case, we have our Eq.5. This result can also be expanded to a composing form with a number of different conditioning variables (Ajay et al., 2023).

E. Assessment of Reward Prediction

In this section, we analyze the reward generation ability of the DDR-II model and compare our model with an MLP generator to show that our model has a better reward generating performance. We evaluate the mean MSE error of the predicted reward and the true reward over the evaluating batch \mathcal{D}_B via the metric:

$$M = \mathbb{E}_{s, s', r \sim \mathcal{D}_B} (D_{\theta'}^2(s, s') - r)^2 \quad (12)$$

We compare our generator with 2-layered MLP generator with 256 hidden units and a WGAN with 2-dimensional latent space and 256 hidden units on the D4RL Hopper Medium-Expert dataset. The results are shown in Figure 5.

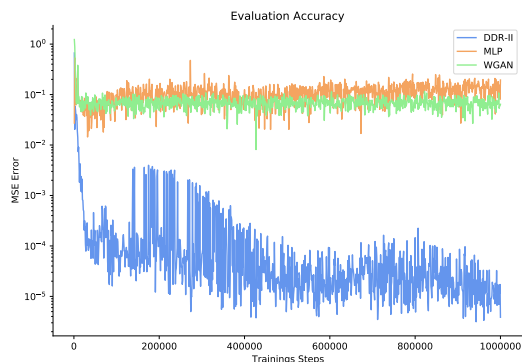


Figure 5. The reward generation accuracy analysis. We train the DDR-II model on the Hopper-Medium-Expert dataset and evaluate the MSE error of the DDR-II model’s generation during the training process. We compare our results with a simple MLP generator and a WGAN generator.

F. Additional Ablations

We perform ablation studies on the Halfcheetah and Walker2d environments in addition to the ablation study in Section 6. We do extra experiments for trajectory generation and stitching. We can still observe improvements by introducing TSKD method in most of the situations. The ablation results are shown in Figure 6. In most of the cases, our method matches and outperforms the original MBTS method.

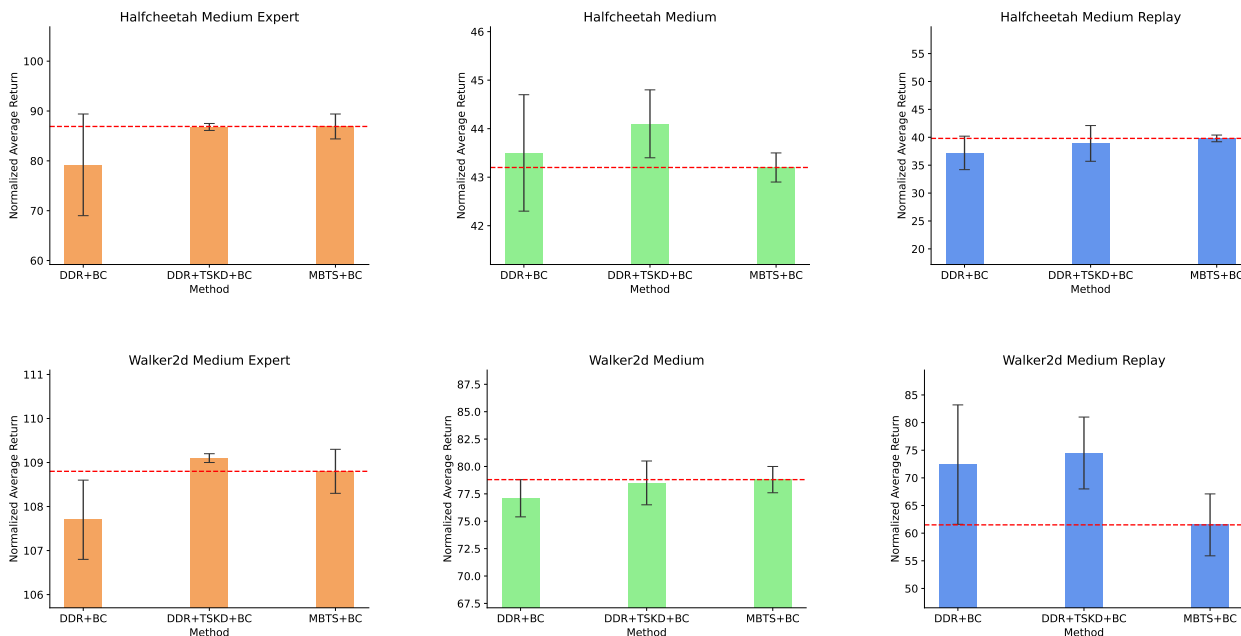


Figure 6. Ablation study on trajectory generation and stitching. The setting is the same as Figure 4, except that the datasets are Halfcheetah (top) and Walker2d (bottom). Difficulty levels are medium expert, medium, and medium replay (left to right).

G. Limitations of Trajectory Stitching Knowledge Distilling

We noticed that in some cases, our method can improve the performance of the BC model to nearly matching or even outperforming our teacher model. But in these cases, the results of our method are much more unstable with high standard

deviation. We think the problem is caused by potential OOD issues when the BC model is saturated and somehow having some tendency to overfit the states with high values. This effect can be reduced by doing trade-off between high performance and stability. For instance, reducing the sum of rewards threshold may help with the stability while slightly suppressing the average sum of episode rewards. Performing stitching with more epochs with more generated trajectories may also be helpful.